Isophoric Arrays—Massively Thinned Phased Arrays with Well-Controlled Sidelobes

David G. Leeper, *Senior Member, IEEE*

***Abstract*— Traditional *filled* phased arrays have an element placed in every location of a uniform lattice with half-wavelength spacing between the lattice points. *Massively thinned* arrays have fewer than half the elements of their filled counterparts. Such drastic thinning is normally accompanied by loss of sidelobe control. This paper describes a class of massively thinned linear and planar arrays that show well-behaved sidelobes in spite of the thinning. The term *isophoric* is derived from Greek roots to denote *uniform weight*. In isophoric arrays, element placement based on *difference* sets forces uniformly weighted spatial coverage. This constraint forces the array power pattern to pass through V uniformly spaced, equal, and constant values that are less than $1/K$ times the main beam peak, where V is the aperture size in half-wavelengths and K is the number of elements in the array. The net result is reduced peak sidelobes, especially when compared to cut-and-try random-placement approaches. An isophoric array will exhibit this sidelobe control even when the array has been thinned to the extent that K is approximately the square root of V. Where more than one beam must be generated at a time, isophoric array designs may be used to advantage even within a traditional filled array. By "interweaving" two isophoric subarrays within a filled array and by appropriate cyclic shifting of the element assignments over time, two independent antenna power patterns can be generated, each with a sidelobe region that is approximately a constant value of $1/(2K)$ relative to the main beam, where K is the number of elements in the subarray.**

***Index Terms*— Array antennas, sidelobe control, sparse array antennas, sub-Nyquist sampling.**

I. Introduction and Summary

TRADITIONAL *filled* phased arrays have an element placed in every location of a uniform lattice with half-wavelength spacing between the lattice points. *Massively thinned* arrays have fewer than half the elements of their filled counterparts. Such drastic thinning is normally accompanied by loss of sidelobe control. This paper describes a class of massively thinned linear and planar arrays that show well-behaved sidelobes in spite of massive thinning. Isophoric arrays derive their sidelobe control from a deterministic placement of elements that achieves a uniform weighting of spatial coverage. The term *isophoric* is based on the Greek roots that denote *uniform weight*.

For a given *aperture size*, massive thinning offers reductions in element count, cost, weight, power consumption, and heat dissipation, albeit with an attendant reduction in antenna gain. In digital-beam-forming arrays, the reduced element count offers reduced computational complexity.

For a *given element count*, thinning offers narrowed beamwidth by making larger apertures possible.

Historically, massive thinning has been accompanied by dramatic loss of sidelobe control. The 1960's and 1970's saw the development of a number of thinning algorithms that attempted to retain some control over sidelobes through deterministic placement of the elements. Success was so elusive that some researchers conjectured *cut-and-try random placement* to be as effective as any deterministic placement algorithm could ever be [1]–[3]. In the 1980's and 1990's, *dynamic programming* and *genetic search algorithms* have fared better [4]–[8] although some of the methods are not appropriate for very large or very highly thinned arrays and the improvements that some of the methods offer are difficult to predict *a priori*.

Rather than using a search algorithm, the approach in this paper attacks the sidelobe control problem directly by applying the properties of *difference sets*, a topic from combinatorial mathematics, to the placement of antenna elements within a regular lattice. These deterministic placements create an *isophoric array* with attendant uniformity of spatial coverage. The uniformity consistently produces, with no searching required, a reduction in peak sidelobe level (PSL) when compared to random element placement.

More specifically, in any linear array of aperture V half-wavelengths, the Nyquist sampling theorem shows that the array power pattern can be completely specified from $2V$ uniformly spaced samples of the pattern. In an isophoric array, the even-numbered samples will necessarily be "locked" to a constant value less than $1/K$ times the main-beam peak, where K is the number of elements in the thinned array. While the odd-numbered samples are not so constrained, the net effect is to produce patterns with much lower PSL's than are typical with cut-and-try random placement.

Isophoric designs apply to linear or planar arrays, whether large or small. While this paper focuses on arrays with 50% thinning, isophoric arrays include arrays thinned to the extent that the number of elements is approximately the square root of the number of elements in their filled counterparts.

Some proposed modern arrays use tens, hundreds, or even thousands of elements combined with digital beam forming (DBF) to produce multiple simultaneous beams. For these arrays, this paper shows how a filled DBF-based array can be operated as two "interwoven" isophoric arrays, thereby reducing the computational complexity in each. In addition,

Manuscript received April 21, 1998; revised July 7, 1999. Parts of this work were supported by AT&T Bell Laboratories Doctoral Support Program.

The author is with the Motorola Personal Networking Group, Scottsdale, AZ 85257 USA.

Publisher Item Identifier S 0018-926X(99)09985-8.

by simple cyclic shifting of the element assignments over time, it is possible to produce power patterns for which the entire sidelobe region is approximately a constant value of $\frac{1}{2}K$ relative to the main beam, where K is the number of elements in the original filled array. In other words, the "peaks" in the sidelobe region virtually vanish.

Sections II–IV of this paper introduce notation and cover basic concepts of difference sets and their application to phased-array design. Sections V and VI contain the main results for linear arrays. Section VII introduces the concept of spatial hopping. Section VIII extends the linear array results to planar arrays.

II. Notation

This section introduces some definitions and notation needed in later sections.

The *array factor* for a linear array of identical isotropic radiators is defined as

$$f(u) = \sum_{m=0}^{V-1} a_m e^{j2\pi m x_0 u} \tag{1}$$

where $a_m = 1$ if an element exists at distance mx_0 wavelengths from the origin and $a_m = 0$, otherwise $u = \sin(\theta)$ is the commonly used direction parameter [9] with θ measured off of a normal to the array, and the lattice has V possible element locations numbered 0 to $V-1$, uniformly spaced at intervals of x_0 wavelengths.

The corresponding array factor for a planar array on a uniform x, y lattice with x_0, y_0 wavelength spacing is

$$f(u,v) = \sum_{m=0}^{V_x-1} \sum_{n=0}^{V_y-1} a_{m,n} e^{j2\pi(mx_0 u + ny_0 y)} \tag{2}$$

where $a_{m,n} = 1$ if an element exists at location (mx_0, ny_0) wavelengths relative to the origin and $a_{m,n} = 0$, otherwise, $u = \sin(\theta)\ \cos(\phi)$ and $v = \sin(\theta)\ \sin(\phi)$ are the commonly used direction parameters [9] and the array lattice has $V = V_x V_y$ possible element locations numbered (0, 0) to $(V_x - 1, V_y - 1)$. The angle θ is measured off of a normal to the array plane and ϕ is measured off of the x-axis of the array plane.

To simplify both expressions, steering angles have, without loss of generality, been set to zero. As usual, applying an appropriate linear phase variation across the elements will allow the main beam to be steered.

Array power patterns for linear and planar arrays are represented as

$$\begin{aligned} ff^*(u) &\equiv f(u) \cdot f^*(u) = |f(u)|^2 \\ ff^*(u,v) &\equiv f(u,v) \cdot f^*(u,v) = |f(u,v)|^2. \end{aligned} \tag{3}$$

Since the array factor and power pattern are *periodic* as well as bandlimited, a finite number of samples, taken from a single period, are sufficient to regenerate the entire factor or pattern over all u. The derivations of the sampling theorem for $f(u)$ and $ff^*(u)$ are straightforward but lengthy and are covered elsewhere [10], [11]. For later reference in this paper, the results for linear and planar arrays are listed below[1]

$$f(u) = \sum_{n=0}^{V-1} f\left(\frac{n}{Vx_0}\right) \frac{\sin\left[\pi V x_0\left(u - \frac{n}{Vx_0}\right)\right]}{V\ \sin\left[\pi x_0\left(u - \frac{n}{Vx_0}\right)\right]} \tag{4a}$$

$$ff^*(u) = \sum_{n=0}^{2V-1} ff^*\left(\frac{n}{2Vx_0}\right) \frac{\sin\left[2\pi V x_0\left(u - \frac{n}{2Vx_0}\right)\right]}{2V\ \tan\left[\pi x_0\left(u - \frac{n}{2Vx_0}\right)\right]}. \tag{4b}$$

Note that while it takes $2V$ samples to specify the power pattern $ff^*(u)$, it takes only V samples to specify the array factor $f(u)$. The reason is that the samples of $f(u)$ are complex, while those of $ff^*(u)$ are real. Having both a real and imaginary part, each sample of $f(u)$ contains twice the information of $ff^*(u)$ sample. Thus, both $f(u)$ and $ff^*(u)$ are completely specified by $2V$ numbers. The sampling theorem shows that at least $2V$ numbers are required to specify either $f(u)$ or $ff^*(u)$. Conversely, both have, at most, $2V$ degrees of freedom in that one can arbitrarily specify only $2V$ sample points in the power pattern. In particular, control over the power pattern is equivalent to and limited to control of the $2V$ sample points.

The corresponding forms for planar arrays are

$$\begin{aligned} f(u,v) = \sum_{m=0}^{V_x-1} \sum_{n=0}^{V_y-1} & f\left(\frac{m}{V_x x_0}, \frac{n}{V_y y_0}\right) \\ & \cdot \frac{\sin\left[\pi V_x x_0\left(u - \frac{m}{V_x x_0}\right)\right]}{V_x\ \sin\left[\pi x_0\left(u - \frac{m}{V_x x_0}\right)\right]} \\ & \cdot \frac{\sin\left[\pi V_y y_0\left(v - \frac{n}{V_y y_0}\right)\right]}{V_y\ \sin\left[\pi y_0\left(v - \frac{n}{V_y y_0}\right)\right]} \end{aligned} \tag{5a}$$

$$\begin{aligned} ff^*(u,v) = \sum_{m=0}^{2V_x-1} \sum_{n=0}^{2V_y-1} & ff^*\left(\frac{m}{2V_x x_0}, \frac{n}{2V_y y_0}\right) \\ & \cdot \frac{\sin\left[2\pi V_x x_0\left(u - \frac{m}{2V_x x_0}\right)\right]}{2V_x\ \tan\left[\pi x_0\left(u - \frac{m}{2V_x x_0}\right)\right]} \\ & \cdot \frac{\sin\left[2\pi V_y y_0\left(v - \frac{n}{2V_y y_0}\right)\right]}{2V_y\ \tan\left[\pi y_0\left(v - \frac{n}{2V_y y_0}\right)\right]}. \end{aligned} \tag{5b}$$

[1]The form for $f(u)$ is valid for V an odd integer. When V is even, the sine function in the denominator must be replaced by a tangent function.

TABLE I
ILLUSTRATION OF THE DIFFERENCE SET PROPERTY FOR DIFFERENCE SET D_2

i	j	$(d_i\text{-}d_j) \bmod V$
0	1	(0-3) mod 7 = 4
0	2	(0-5) mod 7 = 2
0	3	(0-6) mod 7 = 1
1	0	(3-0) mod 7 = 3
1	2	(3-5) mod 7 = 5
1	3	(3-6) mod 7 = 4
2	0	(5-0) mod 7 = 5
2	1	(5-3) mod 7 = 2
2	3	(5-6) mod 7 = 6
3	0	(6-0) mod 7 = 6
3	1	(6-3) mod 7 = 3
3	2	(6-5) mod 7 = 1

III. DIFFERENCE SETS

Difference sets and their associated *block designs* are a branch of combinatorial theory [12]. This section contains a brief introduction to the theory and properties of difference sets.

By definition, a (V, K, Λ) difference set[2] is a set of K unique integers

$$D = \{d_0, d_1, \cdots, d_{K-1}\}, \quad \text{with } 0 \le d_i \le (V-1)$$

such that for any integer $1 \le \alpha \le (V-1)$

$$d_i - d_u = \alpha \,(\text{mod } V), \qquad i \ne j \tag{6}$$

has exactly Λ solution pairs (d_i, d_j) from the set $\{D\}$, where "mod V" means the difference is to be taken modulo V.

Examples of difference sets are

$$\begin{aligned}
&D_1 = \{1,2,4\}; && V=7, K=3, \Lambda=1\\
&D_2 = \{0,3,5,6\}; && V=7, K=4, \Lambda=2\\
&D_3 = \{0,1,3,9\}; && V=13, K=4, \Lambda=1\\
&D_4 = \{1,4,5,6,7,9,11,16,17\}; && V=19, K=9, \Lambda=4\\
&D_5 = \{0,1,2,3,\cdots,(N-1)\}); && V=N, K=N, \Lambda=N.
\end{aligned} \tag{7}$$

The last difference set D_5 is considered "trivial" in the theory of difference sets. As will be seen later, this set will correspond to a traditional "filled" phased array.

While three parameters are used to describe a difference set, only two of the parameters are independent. Since there are $K(K-1)$ possible differences $(d_i - d_j)$ with i not equal to j and since each of the $(V-1)$ possible unique differences is to appear exactly Λ times, it follows that

$$K(K-1) = \Lambda(V-1). \tag{8}$$

As an example, consider the above set $D_2 = \{0,3,5,6\}$ for which $V=7, K=4, \Lambda=2$. As shown in Table I, each of the $V-1=6$ possible unique differences appears exactly $\Lambda=2$ times and since $K=4$, (8) is also satisfied.

[2] In the literature on difference sets, the parameter notation used is universally (v, k, λ). In this paper, the correpsonding notation is (V, K, Λ) in order to avoid confusion with planar array direction parameter v and the familiar wavelength parameter λ.

Given a (V, K, Λ) difference set D, the set

$$D' = \{d_0 + s, d_1 + s, d_2 + s, \cdots, d_{k-1} + s\} \equiv D + s \tag{9}$$

where each element is taken modulo V, will also be a (V, K, Λ) difference set. In this case, D' is called a *cyclic shift* of D. If D_p and D_q are two difference sets with the same parameters (V, K, Λ) and $D_p = tD_q + s$ for any integers t and s with t prime to V (that is, t and V have no common factors), then D_p and D_q are called *equivalent* difference sets. Note that in the examples (7), $D_1 + D_2 = D_5$. For this reason, D_1 and D_2 are *complementary*. If D is a (V, K, Λ) difference set, then its complement D^* will be a difference set with parameters $(V, V-K, V-2K+\Lambda)$.

For any particular (V, K, Λ) satisfying (8) there may be no difference sets, one difference set (disregarding equivalent sets), or several nonequivalent difference sets. Proofs of existence and nonexistence are of great concern to theoreticians. For now, it is sufficient to note that the sets are abundant, that tables of the sets exist, and that construction algorithms [12]–[14] can be used to create them. In particular, construction algorithms exist for sets with $K/V \approx \frac{1}{2}, \frac{1}{4}, \frac{1}{8}$, where K/V is defined herein as the *thinning factor*. It is also possible to construct *very* highly thinned *Singer* difference sets for which K is approximately the square root of V.

IV. DIFFERENCE SETS, AUTOCORRELATIONS, AND LINEAR ARRAYS

From a difference set D, we may construct a sequence or "array" of ones and zeros

$$A_V = \{a_i\} \qquad i = 0, 1, \cdots, V-1$$

where $a_j = 1$ if j is in D and $a_j = 0$ if j is not in D. For example, set D_3 above gives rise to $A_V = \{1\,101\,000\,001\,000\}$. If we create an *infinite* array of ones and zeros

$$A_I = \{\cdots, a_{-2}, a_{-1}, a_0, a_1, a_2, \cdots\}$$

by periodically repeating A_V, we may define an autocorrelation for A_I given by

$$C_I(\tau) = \sum_{n=0}^{V-1} a_n a_{n+\tau}. \tag{10}$$

It follows that if and only if A_I is formed from a difference set [15], then

$$C_I(\tau) = \begin{cases} K, & \text{if } \tau(\text{mod } V) = 0 \\ \Lambda, & \text{otherwise.} \end{cases} \tag{11}$$

In other words, the autocorrelation function is *two-valued*. Ultimately, it is this property that makes the difference set an effective prescription for the design of thinned arrays.

As shown in the next section, by tying the one's and zero's to element locations in a lattice, a periodically repeating element placement sequence dictated by difference sets necessarily has an array power pattern with all sidelobe peaks constrained to be at an identical fixed level that is less than $1/K$ times the main lobe peak. When the infinite sequence is

truncated to a single period, these same fixed levels remain, tying down half the sample points of the power pattern. The PSL of the resulting pattern is then determined by the remaining sample points.

V. Linear Isophoric Arrays

From any sequence of one's and zero's we can construct a corresponding linear phased array by starting with an empty lattice of element locations spaced $\frac{1}{2}$-wavelength apart, placing an element at each location where the sequence has a "1," and skipping each location where the sequence has a "0." From such a construction we can form an array element location function

$$A_I(x) = \sum_{n=-\infty}^{\infty} a_n \delta(x - nx_0) \tag{12}$$

for an infinite length array, where $\delta(x)$ is the usual Dirac delta function, and x_0 is the interelement spacing. Typically, $x_0 = \frac{1}{2}$ wavelength.

While an infinite length array is of no practical interest, a study of its properties will lead to the central result for isophoric arrays. As with any array, the power pattern for this array will be the Fourier transform of the autocorrelation function of the location function. From (11), the autocorrelation function of isophoric array $A_I(x)$ is given by

$$C_I(\chi) = (K - \Lambda) \sum_{n=-\infty}^{\infty} \delta(\chi - nVx_0) + \Lambda \sum_{n=-\infty}^{\infty} \delta(\chi - nx_0). \tag{13}$$

This sum represents an infinite train of impulses at $\chi = 0$, $\pm x_0$, $\pm 2x_0$, $\cdots$. All the impulses have area Λ except for those at $\chi = 0$, $\pm Vx_0$, $\pm 2Vx_0$, $\cdots$ which have area $(K-\Lambda)+\Lambda = K$.

We recall that the Fourier transform of an infinite train of unity-area impulses at $x = 0$, $\pm x_0$, $\pm 2x_0$, $\cdots$ is itself an infinite train of impulses in u, each with area $1/x_0$ located at $u = 0$, $\pm 1/x_0$, $\pm 2/x_0$, $\cdots$. From this it follows that the Fourier transform of autocorrelation $C_I(\chi)$ is

$$ff_I^*(u) = (K - \Lambda) \frac{1}{Vx_0} \sum_{n=-\infty}^{\infty} \delta\left(u - \frac{n}{Vx_0}\right) + \Lambda \frac{1}{x_0} \sum_{n=-\infty}^{\infty} \delta\left(u - \frac{n}{x_0}\right). \tag{14}$$

Using (8) we can eliminate Λ and create a normalized $\overline{ff_I^*(u)}$ by writing

$$\overline{ff_I^*(u)} = \frac{ff_I^*(u)}{K^2} = \rho\left[\frac{1}{Vx_0} \sum_{n=-\infty}^{\infty} \delta\left(u - \frac{n}{Vx_0}\right)\right] + (1-\rho)\left[\frac{1}{x_0} \sum_{n=-\infty}^{\infty} \delta\left(u - \frac{n}{x_0}\right)\right] \tag{15}$$

where

$$\rho = \frac{1}{K}\left[1 - \frac{(K-1)}{(V-1)}\right]. \tag{16}$$

This normalized power pattern has a "main-lobe" impulse with an area of 1 at $u = 0$, $\pm 1/x_0$, $\pm 2/x_0$, $\cdots$, and identical "sidelobe" impulses with area ρ located at $u = \pm 1/Vx_0$, $\pm 2/Vx_0$, $\cdots$.

A finite-length isophoric array will have element location function

$$A_T(x) = \sum_{n=0}^{V-1} a_n \delta(x - nx_0). \tag{17}$$

$A_T(x)$ is therefore a single "truncated" cycle of the infinite length array in (12). Let $ff_I^*(u)$ and $ff_T^*(u)$ be array power patterns for the infinite and finite arrays, respectively. Then a basic property of the Fourier transform permits us to write

$$ff_I^*(u) = ff_T^*(u) \cdot \frac{1}{Vx_0} \sum_{n=-\infty}^{\infty} \delta\left(u - \frac{n}{Vx_0}\right). \tag{18}$$

This expression shows that $ff_I^*(u)$ and $ff_T^*(u)$ are "tied together" at $u = 0, \pm 1/(Vx_0), \pm 2/(Vx_0), \cdots$. It is sometimes said that $ff_T^*(u)$ forms an "envelope" for the $ff_I^*(u)$ impulse train. Therefore, the power pattern $ff_T^*(u)$ for an isophoric array must necessarily pass through the fixed points prescribed by (14).

It follows that for an isophoric array

$$\overline{ff_T^*(n/Vx_0)} = \begin{cases} 1, & \text{for } n = 0, \pm V, \pm 2V, \cdots \\ \rho, & \text{for all other } n. \end{cases} \tag{19}$$

Fig. 1 shows the normalized power pattern for a particular isophoric linear array of 32 elements on a 63-slot lattice with uniform $x_0 = \frac{1}{2}$-wavelength spacing. The regularly spaced, dotted points located at $u = 2/63, 4/63, 6/63, \cdots$ are the sample points referred to in (18). At each of these "even-numbered" sample points $\overline{ff^*(u)} = 10 \log_{10}(\rho) \approx -18.06$ dB, illustrating the effects predicted by (18) and (19).

Note that in Fig. 1, the peak at $u = 2$ is simply a repetition of the main beam. From (1), it is straightforward to show that any array in which the elements are constrained to be located at the fixed points of a uniform lattice will necessarily have a power pattern that is periodic in u with period $u_0 = 1/x_0$ as well as being symmetric about any integer multiple of $u = 1/(2x_0)$, where x_0 is the spacing between adjacent lattice points measured in wavelengths.

For comparison, Fig. 2 shows a power pattern for a *random array*[3] of 32 elements on the same aperture. Note that: 1) there is no regularity evident in the dotted points and 2) the PSL for this particular array is approximately 6 dB higher than that for the isophoric array.

More generally, as shown in the Appendix, the expected PSL of the isophoric array will be lower than that of a corresponding random array by

Isophoric PSL reduction (linear array)

$$\approx 3 + 10 \log(1 - K/V)^{-1} \text{ dB}.^4 \tag{20}$$

[3] In this paper, the term *random array* refers to an array in which an element may appear *anywhere* with an aperture with equal likelihood. A *lattice array* is an array in which elements may only appear at uniformly spaced points in the aperture. A random lattice array is an array in which the elements are located at randomly chosen lattice points.

[4] In this paper, "log" means logarithm to base 10, and "ln" means log to base e.

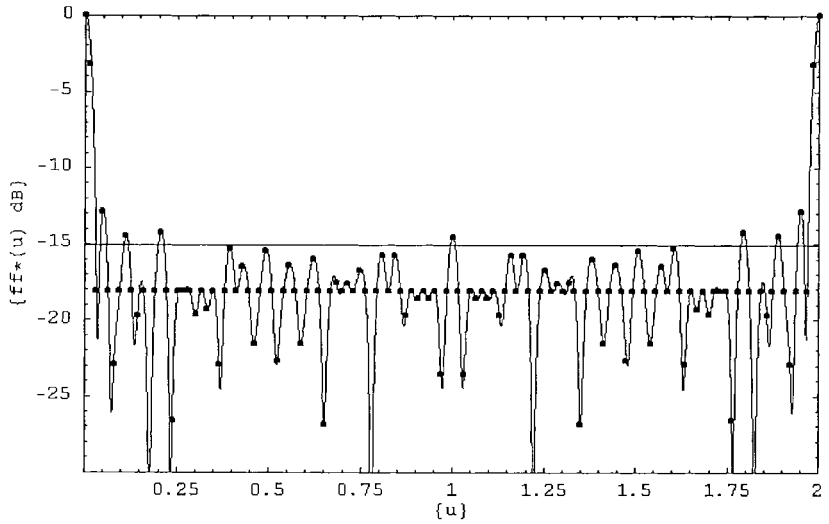

Fig. 1. Isophoric linear-array power pattern. number of elements = 32; aperture size = 62 half-wavelengths.

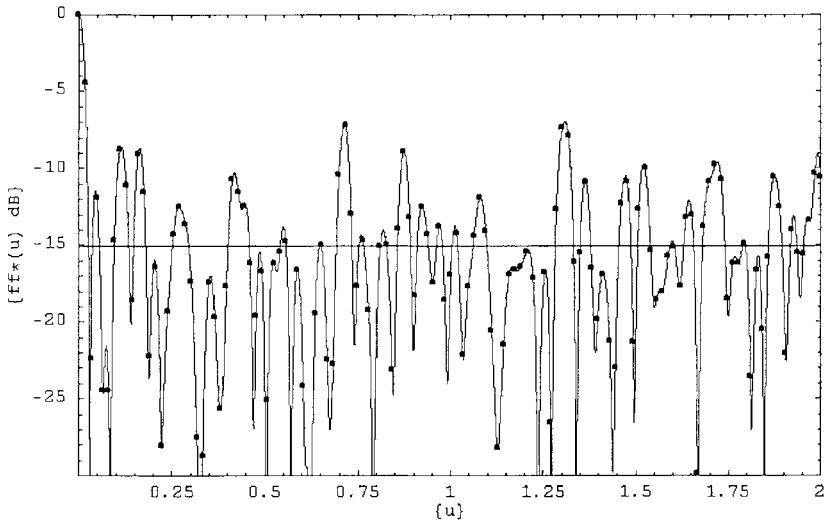

Fig. 2. Random linear array power pattern. Number of elements = 32, aperture = 62 half-wavelengths.

As shown in Section VI, the 3-dB portion of the PSL reduction comes from constraining the locations to those determined by difference sets. The remainder of the improvement comes from simply constraining the elements locations to the points of a fixed lattice. Note that this latter improvement becomes vanishingly small with increased thinning; that is, as K/V approaches zero. However, the 3-dB improvement remains even for highly thinned arrays.

The theory of the random array [2], [16]–[18] shows that

$$\overline{ff^*(u)} = 10\ \log(1/K)\ \text{dB} \tag{21}$$

is the average power in the sidelobe region of a random array. Both figures show a reference line at this average level for these arrays, namely at -15.05 dB.

Reference [10] contains additional experimental comparisons and between random and isophoric array PSL's. Results are summarized in Table II. In Table II, PSL values are in decibels above $1/K$, the average (normalized) power level in the random array sidelobe region. As seen in the table, the experimentally observed reductions in isophoric-array PSL versus random-array PSL compare favorably with predicted values from (20).

TABLE II
EXPERIMENTAL RESULTS OBTAINED FOR THE REDUCTION IN PEAK SIDELOBE LEVEL OFFERED BY ISOPHORIC ARRAYS WHEN COMPARED TO EQUIVALENT RANDOM ARRAYS

	V	K	Thinning K/V	Random PSL (dB)	Isophoric PSL (dB)	PSL Reduction (dB)
Array 1	63	32	~1/2	7.8	0.8	7.0
Array 2	511	256	~1/2	9.1	2.2	6.9
Array 3	85	21	~1/4	8.0	3.1	4.9
Array 4	400	57	~1/8	8.7	5.0	3.7
Array 5	9507	98	~.01	9.7	6.6	3.1

Of course, PSL's for the random array may be reduced by cut-and-try variations in element placement. However, the random array theory shows that the PSL has a standard deviation of about $1\frac{1}{4}$ dB about its expected value. Therefore

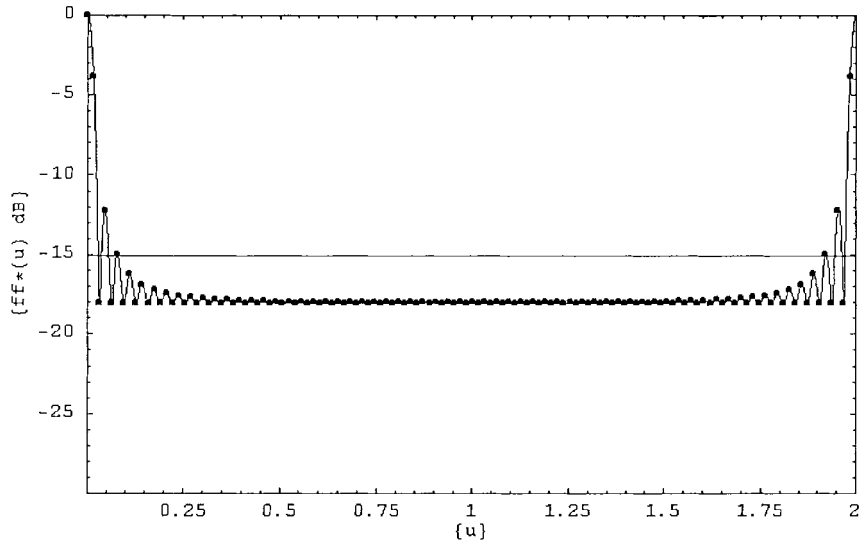

Fig. 3. Expected power pattern of isophoric array with $V = 63$ and $K = 32$.

it would take a great many random array evaluations before one could expect an array to have a PSL as low as a typical isophoric array.

VI. Expected Power Pattern of a Linear Isophoric Array

Isophoric array PSL's in the preceding section could be reduced still further by trying various *cyclic shifts* of the difference set that was used to generate the initial array. A cyclic shift of a difference set $\{D\}$ simply adds an integer s to each member of $\{D\}$ and then reduces each result modulo V. Clearly, there are V unique such shifts possible for $s = 0, 1, \cdots V - 1$. This is a relatively small number to apply in a "cut-and-try" attempt at lowering PSL.

More importantly, as shown in this section, the average power pattern of an isophoric array, taken over all V cyclic shifts of the underlying difference set, is exactly the same as the average power pattern of all $V!/K!/(V-K)!$ possible arrays that one could create by placing K elements on a lattice with V slots. As shown in Section VII, this has some interesting implications for modern arrays which form multiple simultaneous beams.

The expected (average) power pattern of a linear isophoric array is defined as

$$E[ff^*(u)] \equiv ff_E^*(u) = \frac{1}{V} \sum_{s=0}^{V-1} ff_s^*(u) \tag{22}$$

where $ff_s^*(u)$ is the power pattern generated by an array whose underlying difference set has undergone a cyclic shift of s units.

As shown below,

$$\overline{ff_E^*(u)} = \rho + (1-\rho)\,\frac{\sin^2 \pi u V x_0}{V^2 \sin^2 \pi u x_0}. \tag{23}$$

The derivation of this result is straightforward but lengthy. To conserve space, we simply outline the steps as follows.

1) Note that as with any power pattern, each $ff_s^*(u)$ is the Fourier transform of the autocorrelation of the element location function of the array built from a cyclic shift s of the underlying difference set.
2) By substituting the Fourier transform expression for each $ff_s^*(u)$ in (22) and interchanging the order of summation and integration, the average Fourier transform of the V power patterns becomes the Fourier transform of the average of the V autocorrelations.
3) As shown in the Appendix, fundamental properties of difference force the average autocorrelation to be

$$C_E(\tau x_0) = \begin{cases} k\delta(0) & \tau = 0 \\ (V - |\tau|)\,\dfrac{k(k-1)}{v(v-1)}\,\delta(x - \tau x_0), & \text{for } 0 < |\tau| < V \\ 0 & |\tau| \geq V. \end{cases} \tag{24}$$

4) The (normalized) Fourier transform of $C_E(\tau x_0))$ is $\overline{ff_E^*(u)}$, as given by (23).

Note that for a moderately large V, (say, greater than 30), $K/V < \frac{1}{2}$ and u not close to zero (that is, the sidelobe region), the contribution to be made by the second term in (23) is quite small. Under these conditions

$$\overline{ff_E^*(u)} \approx \rho \equiv \frac{1}{K}\left[1 - \frac{(K-1)}{(V-1)}\right]. \tag{25}$$

That is, the power pattern is approximately a constant! Fig. 3 shows for the $(V, K, \Lambda) = (63, 32, 16)$ family of isophoric linear arrays. As seen, the sidelobe pattern is so smooth that it is almost meaningless to speak of a PSL.

In the special case $K = V$, the array is filled and the expression reduces to the well-known power pattern of a filled array. The filled array is in fact a special case of an isophoric array, corresponding to the "trivial" difference set D_5 (7).

As shown in the Appendix, (23) also represents the grand average power pattern of all $V!/K!/(V-K)!$ possible placements of K elements on a V-slot lattice. One way of viewing

the V cyclic shifts of an isophoric array is that they represent a small set of arrays whose average power pattern is the same as the average pattern of the much larger set of all possible of K elements on a V-slot lattice. In the example used thus far, the 63 cyclic shifts of Array 1 have an average power pattern identical to that of the 9.16×10^{17} possible placements of 32 elements on a 63-slot lattice.

Note also that while the average sidelobe power of a random array is $1/K$, the average power of a random *lattice* array is $(1/K)[1-(K-1)/(V-1)] \approx (1/K)(1-K/V)$. Thus, simply constraining the element placements to lattice positions reduces sidelobe levels to some extent, although the improvement becomes vanishingly small with increased thinning. As stated in Section V, further constraining the element placements to be those dictated by a difference set produce another 3 dB of expected PSL reduction. This 3-dB reduction is independent of how much the array has been thinned.

VII. Complementary Isophoric Arrays with "Spatial Hopping"

While the sidelobe characteristics of $ff_E^*(u)$ would make it a desirable power pattern for many purposes, no single static array placement can produce it. However, using simple digital beam forming (DBF) techniques, it is possible to operate a filled array as two independent complementary isophoric arrays, each of which has the "ideal" $ff_E^*(u)$ pattern. The technique, herein called "spatial hopping," is as follows.

1) Begin with a filled array with V slots and $K = V$ elements.
2) Choose a difference set D_P with parameters (V, K_P, Λ_P). For example, the (63, 32, 16) difference set that generates the pattern in Fig. 1 is

$$DP = \{0,5,6,10,12,15,16,17,18,20,24,25,26,29,32,34,35,37,38,39,41,42,45,46,48,50,52,53,54,55,56,57\}.$$

3) At time $t = 0$, designate isophoric array A_P to be the elements whose positions are listed in D_P.
4) From D_P, generate the complementary difference set D_Q, whose element positions are all of those that not in D_P. Set D_Q will have $(V, K_Q, \Lambda_Q) = (V, V-K_P, V-2K_P+\Lambda_P)$. Continuing the example above

$$DQ = \{1,2,3,4,7,8,9,11,13,14,19,21,22,23,27,28,30,31,33,36,40,43,44,47,49,51,58,59,60,61,62\}.$$

5) At time $t = 0$, designate isophoric array A_Q to be the elements whose positions are listed in D_Q.
6) At each sample time thereafter, spatially "hop" the array element assignments by adding integer s to each member of the underlying difference sets, reducing the result modulo V. Integer s can be one or any other integer that shares no common factors with V.

The result will be two independent arrays, each of whose power patterns is given by (23) and illustrated for the example above in Fig. 3. This pattern retains the original beamwidth (angular privacy) of the full aperture-filled array and has an ideal (nearly flat) sidelobe region. Each of the two arrays would, however, suffer a 6-dB loss in absolute gain when compared to the original filled array.

In some applications, it may be advantageous to trade absolute gain for reduced power consumption or increased speed of computation by temporarily operating a filled array as a single hopped subarray. In other applications, where two subbeams must be formed simultaneously, splitting a filled array into two independent subarrays may be computationally simpler and faster than generating two beams with digital beamforming (DBF) computations. Finally, in applications where more than two beams are needed, splitting the computation into two independent antennas may be computationally faster than that for one array of twice the size. This is particularly true for antennas with hundreds or thousands of elements.

VIII. Extensions to Planar Arrays

Isophoric arrays, both static and spatially hopped, can be planar as well as linear. The principals are the same. We seek a deterministic placement of K elements in a rectangular lattice such that the element location function has a two-level autocorrelation function in two dimensions.

The element location function for a planar array is defined by

$$A_T(x,y) = \sum_{m=0}^{V_x-1} \sum_{n=0}^{V_y-1} a_{m,n}\delta(x-mx_0, y-ny_0) \tag{26}$$

where the array has dimensions V_xV_y, $\delta(x-g, y-h)$ is interpreted as a unit impulse at location $(x,y) = (g,h)$, and the coefficients form a V_x-by-V_y matrix of ones and zeros that designate the presence or absence of an array element at (mx_0, ny_0).

Analogous to (10), we form a two-dimensional autocorrelation for an infinitely repeated version $A_I(x,y)$ of $A_T(x,y)$ as

$$C_I(p,q) = \sum_{m=0}^{V_x-1} \sum_{n=0}^{V_y-1} a_{m,n}a_{m+p,n+q}. \tag{27}$$

We let the number of ones in the $a_{m,n}$ coefficients equal K and assume that we can discover a placement of ones and zeros such that

$$C_I(p,q) = \begin{cases} K, & \text{if } V_x \text{ divides } p \text{ and } V_y \text{ divides } q \\ \Lambda, & \text{otherwise.} \end{cases} \tag{28}$$

That is, $A_I(x,y)$ has a two-level autocorrelation function. If this can be done, then we know that all the V_xV_y sample points in the sidelobe region of $f(u,v)$ (5) will necessarily have magnitude K. We also know that the even-numbered samples from the sidelobe region of $ff^*(u,v)$ will have magnitude K^2. The odd-numbered samples will be the ones that determine the PSL.

Results from Monte Carlo simulations [10] show that compared to a random (nonlattice) placement of elements on the

TABLE III
EXAMPLE OF HOW A 9× 7 PLANAR ARRAY CAN BE CONSTRUCTED FROM A (63,32,16) DIFFERENCE SET

				a_{13}		a_6		
	(etc)		a_{12}		a_5			
a_{18}		a_{11}		a_4				
	a_{10}		a_3					a_{17}
a_9		a_2					a_{16}	
	a_1					a_{15}		a_8
a_0					a_{14}		a_7	

same aperture, a static (not spatially hopped) isophoric array will have an expected improvement in PSL of

$$\text{Planar Array Isophoric PSL Reduction} \approx 1.5 + 10\ \log_{10}(1 - K/V)^{-1}\ \text{dB} \tag{29}$$

where $V = V_x V_y$. This improvement is 1.5 dB smaller than it was for linear arrays. (See Appendix for further discussion.)

As with linear arrays, if we can find a placement algorithm with the property described by (28), then we can spatially hop the array element assignments as we did for linear arrays, thereby guaranteeing a fixed low-sidelobe power pattern for $ff^*(u,v)$ as we did for $ff^*(u)$. One algorithm that works [19] is as follows.

Assume we have a linear sequence of V ones and zeros

$$A_V = \{a_i\}, \qquad i = 0, 1, \cdots, V-1$$

dictated by a difference set as in (6). Then the assignment

$$a_{m,n} = a_i \quad \text{where } m = i \ (\text{mod } V_x) \quad \text{and} \quad n = i \ (\text{mod } V_y), \qquad i = 0, 1, \cdots, V-1 \tag{30}$$

will create a rectangular array of ones and zeros

$$A_{V_x V_y} = \{a_{m,n}\} \quad m = 0, 1, 2, \cdots, V_x - 1 \qquad n = 0, 1, 2, \cdots, V_y - 1 \tag{31}$$

that has the desired two-level autocorrelation function.

For example, the (63, 32, 16) difference set would be placed in a 9×7 array as shown in Table III. As shown, a_0 is placed in the "southwest" corner of the array and each succeeding coefficient is placed in the slot to the "northeast," continuing from the other side whenever an edge is reached until the entire $V = V_x V_y = (9)(7) = 63$ coefficients have been placed. The table shows the placement of the first 18 coefficients. An antenna element will be placed in each location where $a_i = 1$ and not placed where $a_i = 0$. Additional discussion may be found in [19].

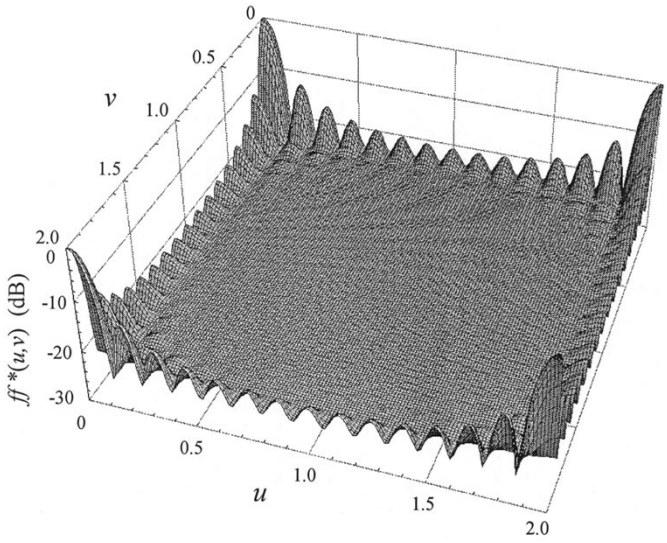

Fig. 4. Expected power pattern of isophoric planar array with $V = V_x V_y = 15 \times 17$ half-waves and $K = 128$ elements. This exact pattern is realizable with "spatial hopping." Note pattern floor at $10 \log \rho = -24$ dB.

With the approach above, we can create a static isophoric array with expected power pattern

$$\overline{ff_E^*(u,v)} = \rho + (1-\rho) \cdot \frac{\sin^2 \pi u V_x x_0}{V_x^2 \sin^2 \pi u x_0} \cdot \frac{\sin^2 \pi v V_y y_0}{V_y^2 \sin^2 \pi v y_0}. \tag{32}$$

As with linear arrays, once we move into the sidelobe region (that is, u and v not too close to 0, ± 2, ± 4, $\cdots$), the expected normalized pattern is approximately the constant ρ, where ρ is given by (15). Fig. 4 shows for a $\overline{ff_E^*(u,v)}$-slot lattice, with 128 elements.

Note that for the special case $V = K$, ρ becomes zero and $\overline{ff_E^*(u,v)}$ becomes the power pattern of the familiar filled rectangular-lattice array. Note also that the beamwidth implied by (32) is independent of the thinning factor $\beta = K/V$. Even a very highly thinned isophoric array will have the same beamwidth as a filled array.

Again, as with linear arrays, if we begin with a filled lattice and operate it as two independent interwoven isophoric arrays with spatially hopped element assignments, we can actually achieve two independent patterns obeying $\overline{ff_E^*(u,v)}$ on a time-averaged basis.

In modern multibeam arrays with digital beam forming, computational complexity tends to grow as the *square* of the number of elements. Some of the arrays contemplated for space applications have thousands of elements, creating a huge computation-speed challenge. For such cases, the results of this section show that the computation burden can be reduced by operating the array as two independent isophoric spatially hopped arrays. Each of the arrays will have the narrow beamwidth (angular privacy) of the original filled array and each will have the well-behaved sidelobe pattern implied by (32) and shown (by example) in Fig. 4.

IX. Conclusions and Open Issues

This paper has described a class of massively thinned linear and planar phased arrays called *isophoric arrays*. Isophoric arrays have element locations that are constrained by an algorithm based on *difference sets*, a topic from combinatorial mathematics. These constraints produce arrays with PSL's demonstrably better than those obtainable with simple cut-and-try placement techniques, as well as many previously published algorithmic techniques.

Isophoric designs may be useful even in traditional filled arrays when more than one beam must be formed. In particular, a technique called *spatial hopping* is introduced that can produce two independent beam patterns from a single filled array. While each of these beams will have 6 dB less gain than the original filled array, each will retain the narrow beamwidth of the original array and each will have a power pattern with a virtually perfect ("flat") sidelobe region.

A detailed comparison of isophoric arrays with those derived from the most recent genetic algorithms and dynamic programming is left as a future research issue. It may be profitable to *combine* the two approaches in some way such as by using isophoric arrays as the initial array in the search algorithms.

Appendix

Derivation of (20): From examination of Fig. 1, it is evident that the peak sidelobe (PSL) behavior of the isophoric array is determined by the behavior of the odd-numbered sample points of the power pattern $ff^*(u)$ as it is defined in (4b).

By defining $u_m = m/Vx_0$ and $u_m + \frac{1}{2} = (m+\frac{1}{2})/Vx_0$, $m = 0, 1, \cdots, V-1$, and by using the sampling expansion of (4a), the array factor representation for these PSL-determining points may be written as

$$f(u_{m+(1/2)}) = \sum_{n=0}^{V-1} f(u_m)\, \frac{\sin[\pi(m-n+\frac{1}{2})]}{V\,\sin[\pi(m-n+\frac{1}{2})/V]} \quad \text{for } m = 0, 1, \cdots, V-1. \tag{33}$$

From (5) and (19), for an isophoric array, $f(u_0) = K$, and

$$f(u_m) = K\rho^{1/2} e^{j\phi_m}, \quad \text{for } m = 1, 2, \cdots, V-1. \tag{34}$$

That is, if and only if the array is isophoric, all of these points have identical fixed magnitude $K\rho^{1/2}$ and some phase angle ϕ_m. Applying (34) and a simple trigonometric identity allows

$$f(u_{m+(1/2)}) = K\left[\frac{(-1)^m}{V\,\sin[\pi(m+\frac{1}{2})/V]} + \sum_{n=1}^{V-1} \frac{(-1)^{m-n}\rho^{1/2} e^{j\phi_m}}{V\,\sin[\pi(m-n+\frac{1}{2})/V]}\right]. \tag{35}$$

For the cases of interest, V is moderately large (greater than 50) and K is approximately $V/2$ or less. Note that in (35), the terms with the largest magnitude will be those for which $n = m$ and $n = m+1$. The magnitude of those two terms is approximately $2\rho^{1/2}/\pi$. The *sidelobe region* of $f(u)$ is defined herein as that region of u for which $2\rho^{1/2}/\pi$ exceeds the magnitude of the first term in brackets in (35). By simple algebra, this implies

$$\text{sidelobe region} \approx \frac{1}{2Vx_0\rho^{1/2}} < u < \frac{1}{x_0}\frac{1}{2Vx_0\rho^{1/2}}.$$

This is, effectively, the region where the influence of the main beam sample becomes subordinate to the influence of local samples of $f(u)$ (see [2]). For the arrays in Figs. 1 and 2, this interval is approximately $0.12 < u < 1.88$. In the sidelobe region, (35) becomes

$$f(u_{m+(1/2)}) \approx K\rho^{1/2} \sum_{n=1}^{V-1} \frac{(-1)^{m-n} e^{j\phi_n}}{V\,\sin[\pi(m-n+\frac{1}{2})/V]} \quad \text{(sidelobe region)}. \tag{36}$$

The phases ϕ_n are as yet unspecified. They will vary depending on the particular difference set chosen as well as the particular selected cyclic shift of the difference set. While they are deterministic, for purposes of peak sidelobe estimation they may be modeled as independent, identically distributed random variables, uniformly distributed over the interval $(-\pi, \pi)$. It follows that the even-numbered sample points in $ff^*(u)$ may be modeled as the magnitude of the fixed sample points $(K\rho^{1/2})$ times the magnitude of a random variable represented by the summation in (36).

Note again that the most influential terms in the summation are where $n = m$ and $n = m+1$. Note also that the argument of the sine function is quite small in the region of greatest importance. Since $\sin(x)$ is approximately equal to x for small x, the function may be replaced by its argument. Finally, under the assumptions on ϕ_n, the factor $(-1)^{m-n}$ will have no influence on the distribution of the random variable represented by the summation. It may therefore be dropped. Combining these assumptions produces

$$|f(u_{m+(1/2)}| \sim K\rho^{1/2} \sum_{n=1}^{V-1} \frac{e^{j\phi_n}}{\pi(m-n+\frac{1}{2})} \quad \text{(sidelobe region)} \tag{37}$$

where the symbol $\sim$ is to be read "is distributed as." As a final approximation, under the assumption that V is greater than 50 and m can only assume values from the sidelobe region, the dependence on V and m becomes very weak. For convenience, the summation above is assumed equivalent to the complex random variable

$$Z \equiv \sum_{n=-\infty}^{\infty} \frac{e^{j\phi_n}}{\pi(n-\frac{1}{2})}. \tag{38}$$

Finally, using this definition for Z and dividing $ff^*(0)$ by K^2 to force $\overline{ff^*(0)} = 1$

$$\overline{ff^*(u_{m+(1/2)})} \sim \rho|Z|^2. \tag{39}$$

In words, (39) states that the squared magnitude of the even-numbered sample points of $ff^*(u)$ in (4b) is distributed as the

fixed squared magnitude ρ of the odd-numbered sample points times a random multiplier

$$Y \equiv |Z|^2$$

where Z is given by (38).

It is straightforward to show that Y has an expected value of one and a variance of 2/3. But since there are approximately V opportunities for the power pattern to attain a large PSL, the real interest in the expected value of the random variable Y_V, where

$$Y_V \sim \text{largest of } V \text{ samples of } Y.$$

Unfortunately, the cumulative distribution function of Y_V does not appear to exist in closed form. Accordingly, simulations were used [10] to generate the approximation

$$\overline{Y}_V \equiv E[Y_V] \approx 0.8488 + 1.128\ \log(V).$$

The expected PSL for an isophoric array is therefore

$$\begin{aligned}\text{PSL (Isophoric)} &\approx 10\ \log\left[\frac{1}{K}\left(1-\frac{K}{V}\right)\right] \\ &\quad + 10\ \log[0.8488 + 1.128 \log V]\ \text{dB} \end{aligned} \tag{40}$$

relative to the peak of the main beam. The conditions for this approximation to be valid are that $V > 50$ and $K < V/2$.[5]

The theory of the random array [2] shows that the PSL for a random array is (41), shown at the bottom of the page. Numerical and graphical evaluation [10] of these two approximations yields

$$\begin{aligned}&\text{PSL (Random)} - \text{PSL (Isophoric)} \\ &\quad \approx 3 + \log(1 - K/V)^{-1}\ \text{dB}. \end{aligned} \tag{42}$$

This is the result shown in (20). The improvement predicted by this result is borne out in actual test cases, as shown in Table II.

Derivation of (24)

To derive (24), we first note that if $C_E(\tau)$ is the average autocorrelation across the V cyclic shifts of the underlying difference set, then

$$C_S(\tau) = V C_E(\tau) \tag{43}$$

indicates the total number of interelement spacings τ which appear (collectively) in all V cyclic shifts of the underlying difference set D. We know that $(d_I - d_j) \bmod V = \tau$ has exactly Λ solution pairs in the difference set for $0 < \tau < V$. For each such pair there is a cyclic shift $s_o = (V - d_j)$ which will make $d_j = 0$. Then for each such pair, the cyclic shifts $s = s_o, s_o + 1, s_o + 2, \cdots, s_o + (V - \tau - 1)$ will cause the *positive* interelement spacing Λ to appear a total of $(V - \tau)$ times. Since there are Λ such pairs

$$C_S(\tau) = (V - \tau)\Lambda \quad \text{for } 0 < \tau < V.$$

Using (18) to eliminate λ

$$C_S(\tau) = (V - \tau)\frac{K(K-1)}{(V-1)}, \qquad \text{for } 0 < \tau < V. \tag{44}$$

Since this derivation is identical for the symmetric case of *negative* interelement spacings $-V < \tau < 0$, we also have $C_S(-\tau) = C_S(\tau)$. Furthermore, since there are K elements in each of the V cyclic shifts of $D, C_S(0) = KV$. Combining these two observations with (43) and (44) yields (24).

As indicated in Section VI, (24) and consequently (23) also apply to the set of all $V!/K!/(V-K)!$ possible placements of K elements on a V-slot lattice. To show this, we let

$$\begin{aligned} C_S(\tau) &= N(V,K) C_E(\tau) \quad \text{where} \\ N(V,K) &= \binom{V}{K} = \frac{V!}{K!(V-K)!} \end{aligned} \tag{45}$$

replaces V in (43). To begin, we consider that to obtain a spacing of $\tau = (V-1)$, there must be an element at zero and an element at $(V-1)$. The remaining $(K-2)$ elements may be located anywhere within the remaining $(V-2)$ slots. Hence, there are

$$C_S(V-1) = \binom{V-2}{K-2}$$

unique element placements to yield a spacing of $\tau = (V-1)$. Similarly, to obtain a spacing of $\tau = (V-2)$, there must be an element at zero and $(V-2)$ or an element at one and $(V-1)$. Thus

$$C_S(V-2) = 2\binom{V-2}{K-2.}$$

It follows that for $1 < \tau < V$

$$\begin{aligned} C_S(\tau) &= (V-\tau)\binom{V-2}{K-2} \\ &= (V-\tau)\frac{(V-2)!}{(K-2)!(V-K)!}. \end{aligned} \tag{46}$$

Noting the same symmetry as above for negative spacings and the fact that $C_E(0) = K$, we can divide $C_S(\tau)$ by $N(V,K)$ and obtain (24).

[5] The log function argument in the first term is the variable ρ (5-5). Given the conditions on K and V, the approximation has used the simpler K/V to approximate $(K-1)/(V-1)$.

$$\text{PSL (Random)} \approx 10\ \log\left[\frac{1}{K}\right] + 10\ \log\left[1 - \ln(1 - 5^{1/Y}) - \frac{2}{\ln(1 - 5^{1/Y})}\right]\ \text{dB}. \tag{41}$$

Derivation of (29)

Equation (29) for planar arrays may be derived in a manner parallel to that which led to the linear array (20), but starting with the two-dimensional sampling expression given in (5). This (lengthy) process produces the following analog to (37):

$$|f(u_{p+1/2}, v_{q+1/2})| \sim K\rho^{1/2}\left|\sum_{m=1}^{V_x-1}\sum_{n=1}^{V_y-1}\frac{e^{j\phi_{m,n}}}{\pi^2(p-m+\frac{1}{2})(q-n+\frac{1}{2})}\right|. \tag{47}$$

As described in Section VIII, the PSL of the pattern will be determined by the odd-numbered samples of the array power pattern. The behavior of these samples can be estimated in the same manner as for the linear array case, but the derivation is much more lengthy. The planar array equivalent to (47), above, turns out to be

$$Z = \sum_{m=-\infty}^{\infty}\sum_{n=-\infty}^{\infty}\frac{e^{j\phi_{m,n}}}{\pi^2(m-\frac{1}{2})(n-\frac{1}{2})}. \tag{48}$$

Analogous computations show that $E[|Z|^2] = 1$ as in the linear case. However, $\mathrm{Var}[|Z^2|] = 8/9$, which is larger than the value of 2/3 obtained for the linear case. This necessarily implies an increased likelihood of a large PSL. Indeed, Monte Carlo simulations produce the results in (8-4) showing that the 3-dB improvement offered by linear Isophoric arrays reduces to 1.5 dB for planar arrays.

ACKNOWLEDGMENT

The author would like to thank Prof. B. D. Steinberg, University of Pennsylvania, Philadelphia, who introduced him to the problem of sidelobe control in thinned phased arrays. The work on isophoric planar arrays and spatial hopping was stimulated by discussions with S. Ma at the Motorola Satellite Communications Group. The author would also like to thank S. Daniel, J. Locke, and H. Malone, Motorola Space and Systems Technology Group, Chandler, AZ, and especially W. Wu of Consultare, Bethesda, MD, for stimulating discussions on this subject.

REFERENCES

[1] Y. T. Lo and S. W. Lee, "A study of space-tapered arrays," *IEEE Trans. Antennas Propagat.*, vol AP-14, pp. 22–30, Jan. 1966.

[2] B. D. Steinberg, *Principles of Aperture and Array Systems Design*. New York: Wiley, 1976.

[3] ——, "Comparison between the peak sidelobe of the random array and algorithmically designed aperiodic arrays," *IEEE Trans. Antennas Propagat.*, vol AP-21, pp. 366–370, May 1973.

[4] R. L. Haupt, "Thinned arrays using genetic algorithms," *IEEE Trans. Antennas Propagat.*, vol. 42, pp. 993–999, July 1994.

[5] S. Holm, "Properties of the beampattern of weight-layout-optimized sparse arrays," *IEEE Trans. Ultrason., Ferroelect., Frequency Contr.*, vol. 44, pp. 983–991, Sept. 1997.

[6] P. K. Weber, R. M. Schmitt, B. D. Tylkowski, and J. Steck, "Optimization of random sparse 2-D transducer arrays for 3-D electronic beam steering and focusing," in *Proc. IEEE Ulstrason. Symp.*, 1994, vol. 3, pp. 1503–1506.

[7] D. J. O'Neill, "Element placement in thinned arrays using genetic algorithms," *Proc. Oceans'94*, vol. 2, pp. 301–306, Sept. 1994.

[8] A. Trucco, "Synthesis of aperiodic planar arrays by a stochastic approach," in *Proc. Oceans'97*, 1997, pp. 820–825.

[9] E. Brookner, *Practical Phased Array Antenna Systems*. Norwood, MA: Artech House, 1991.

[10] D. G. Leeper, *Sidelobe Control in Sub-Nyquist Sampling*, Ph.D. dissertation, Univ. Pennsylvania, Philadelphia, Elect. Eng. Sci., 1977.

[11] ——, U.S. Patent 4 071 848, "Thinned aperiodic antenna arrays with improved peak sidelobe level control," Jan. 1978.

[12] M. Hall, Jr., *Combinatorial Theory*, 2nd ed. New York: Wiley, 1986.

[13] L. D. Baumert, *Cyclic Difference Sets*. New York: Springer-Verlag, 1971.

[14] W. Wesley Peterson, *Error-Correcting Codes*. Cambridge, MA: MIT Press, 1961.

[15] S. W. Golomb, *Digital Communications with Space Applications*. Englewood Cliffs, NJ: 1964.

[16] Y. T. Lo, "Random periodic arrays," *Radio Sci.*, vol. 3, no. 5, pp. 425–436, May 1968.

[17] ——, "A mathematical theory of antenna arrays with randomly spaced elements," *IEEE Trans. Antennas Propagat.*, vol. AP-12, pp. 257–268, May 1964.

[18] B. D. Steinberg, "The peak sidelobe of the phased array having randomly located elements," *IEEE Trans. Antennas Propagat.*, vol AP-20, pp. 129–136, Mar. 1972.

[19] N. J. A. Sloane and F. J. MacWilliams, "Pseudorandom sequences and arrays," *Proc. IEEE*, vol. 64, pp. 1715–1729, Dec. 1976.

David G. Leeper (S'67–M'77–SM'89) received the B.S, M.S., and Ph.D. degrees in electrical engineering from Washington University, St. Louis, MO, Cornell University, Ithaca, NY, and University of Pennsylvania, Philadelphia, respectively.

He is a Vice President of Technical Staff, Motorola, Scottsdale, AZ. He is currently leading work on short-range low-power high-bandwidth wireless networking of personal electronic devices and their connection to the internet. From 1969 to 1984 he was with ATT Bell Laboratories, Holmdel, NJ, where he worked on digital systems engineering and network performance measurement programs. From 1984 to 1992 he worked at Bellcore (now Telcordia), Red Bank, NJ, where he led programs on new service development and advanced network architectures and technologies. Since 1992 he has been with Motorola, where he has worked on space systems engineering, advanced network architectures, and personal area networking.